Developing biocompatible silver nanoparticles using epigallocatechin gallate for dental use

Yin IX[1], Zhao IS[2], Yu OY [1], Mei ML[1]*, Li QL[3], Chu CH[1]*

[1] Faculty of Dentistry, the University of Hong Kong, Hong Kong, China

[2] School of Stomatology, Shenzhen University Health Science Center, Shenzhen, China

[3] College of Stomatology, Anhui Medical University, Hefei, China

Keywords:

Silver nanoparticles (AgNPs), Epigallocatechin gallate (EGCG), Green chemistry, Antibacterial agent

Correspondence to : * Dr. Mei ML
Faculty of Dentistry
The University of Hong Kong
34 Hospital Road
Hong Kong SAR, China
E-mail: mei1123@hku.hk

* Prof. Chu CH
Faculty of Dentistry
The University of Hong Kong
34 Hospital Road
Hong Kong SAR, China
E-mail: chchu@hku.hk

Abstract

***Objective**: To develop silver nanoparticles (AgNPs) using epigallocatechin gallate (EGCG) and evaluate its biocompatibility and inhibition effect on Streptococcus mutans biofilm growth.*

***Design**: AgNPs were synthesized using EGCG as a reducing agent. Cytotoxicity was assessed using half-maximal inhibitory concentration (IC_{50}) against human gingival fibroblast (HGF-1) and stem cells from human exfoliated deciduous teeth (SHED). Antibacterial properties were evaluated with minimum inhibitory concentration (MIC) and minimum bactericidal concentration (MBC) against S. mutans. Dentine blocks were treated with AgNPs, silver nitrate ($AgNO_3$), or water before being incubated with S. mutans. The kinetics, morphology and viability of the biofilm at different time points were assessed by colony-forming units (CFUs), scanning electron microscopy (SEM), and confocal laser scanning microscopy (CLSM), respectively. Lactic acid and polysaccharide production of the biofilm were also investigated.*

***Results**: Spherical AgNPs with diameter 17 ± 7 nm were developed. The IC_{50} of AgNPs and $AgNO_3$ against HGF-1 were 44.88 ± 11.39 μg/mL and 11.53 ± 6.96 μg/mL, respectively ($p < 0.001$), whereas those against SHED were 68.02 ± 24.48 μg/mL and 9.54 ± 6.63 μg/mL, respectively ($p=0.02$). The MIC of AgNPs and $AgNO_3$ were 32.22 ± 7.34 μg/mL and 48.89 ± 15.11 μg/mL, respectively ($p=0.01$), whereas their MBC was 63.33 ± 11.73 μg/mL and 85.00 ± 20.77 μg/mL, respectively ($p=0.02$). Log CFUs of the AgNPs group were the lowest among the groups ($p < 0.001$). SEM and CLSM found a confluent biofilm in $AgNO_3$ and water groups but not in AgNPs group. Biofilms in AgNPs group was revealed with lowest level of acidic acid and polysaccharides production ($p < 0.001$).*

***Conclusion**: This study developed biocompatible AgNPs which inhibited the growth of a cariogenic biofilm.*

Introduction

In recent years, nanotechnology has emerged in science and technology for the purpose of manufacturing new materials. This technology is defined as the design, characterization, and application of matter with at least one dimension sized from 1 to 100 nm. Nanotechnology has already found practical applications in health and
daily life (Cassee et al. 2011).

Among the various types of nanoparticles, silver nanoparticles (AgNPs) as a kind of metallic nanoparticle have been reported to promise greater biomedical application (Bhattacharya and Mukherjee 2008). AgNPs provide a large surface area for contact with bacteria, which allow the particles to attach to the cell membrane and easily penetrate into the bacteria, thus AgNPs have broad-spectrum antibacterial activities (Wu and Wei 2002). Compared to silver compounds, AgNPs are increasingly used due to their slower dissolution rate, leading to a continuous release of silver ions. In addition, AgNPs provide superior optoelectronic properties to the black stain caused by silver compounds (Ravindran et al. 2013). However, some researchers also raised concern about the toxicity and accumulation effects of AgNPs over time during in vivo use in humans (Durán et al. 2016). A previous study indicated that AgNPs have a size-dependent cytotoxicity, and the mechanism of cytotoxicity was shown to be reactive oxygen species (ROS) (Carlson et al. 2008). Therefore, it is imperative to develop low-toxic AgNPs which provide minimal risks to the users.

Green chemistry is the design, development, and application of chemical products and process to reduce or eliminate the use and generation of substances hazardous to human health and the environment (Moulton et al. 2010). Biopolymers are extensively used as green chemical approaches to develop biodegradable nanoparticles. They are usually used as stabilizers, as well as reducing and capping agents (Chauhan et al. 2016).

Epigallocatechin gallate (EGCG), a natural plant polyphenol extraction from tea, has been known to contain potentially beneficial traits, including antioxidant, antimicrobial, antidiabetic, anti-inflammatory, and cancer preventive properties (Ferrazzano et al. 2011). EGCG contains a large number of phenolic hydroxyls that are able to donate electrons when in contact with

electrophilic ions. Those phenolic hydroxyls endow EGCG's potential capability of reducing Ag^+ into Ag^0 (Hussain and Khan 2014). EGCG is also demonstrated to be a promising bacteria inhibitor due to various biological effects on oral *Streptococci* (Wu and Wei 2002). Chitosan, an N-deacetylation product of chitin, is always used in the design of biomaterials as it has advantageous properties such as biocompatibility, biodegradability, and nontoxicity (Regiel et al. 2012).

The prevalence of root caries is increasing due to extended root exposure time by increased life expectancy and the special anatomical location of the root in the oral cavity (Griffin et al. 2004). A systematic review concluded that about 40% of people older than 70 suffered from untreated root caries (Kassebaum et al. 2015). Dentine on the root surface is soft and porous; bacteria penetrate further into the tissue at an earlier stage of lesion development in root caries (Kidd and Fejerskov 2004). Therefore, AgNPs have potential use in dentistry to prevent biofilm formation on root surface. The aims of the study are twofold: (1) develop novel AgNPs with low toxic effect and high antibacterial effect using EGCG as the reducing agent and chitosan as the capping agent and (2) investigate the inhibitory effect of the AgNPs against *Streptococcus mutans* growth on root dentine surface.

Materials and methods

Synthesis of silver nanoparticles

The synthesis of AgNPs in an aqueous solution was carried out via chemical reduction of silver nitrate ($AgNO_3$) with EGCG as the reducing agent and chitosan as the capping agent. $AgNO_3$ (Gordon Laboratories, Upper Darby, PA, USA) in the amount of 0.5 mL 50mM was mixed with 20 mL chitosan (10 mg/mL, pH=5) (Sigma-Aldrich, St. Louis, MO, USA), which was previously dissolved in 0.2% (v/v) acetic acid. Subsequently, 1 mL 50mM EGCG (Sigma-Aldrich, St. Louis, MO, USA) was added into the mixed solution under continuous stirring. The reaction mixture was stirred for 10 min. to ensure the formation and growth of nanoparticles. AgNPs were washed three times with distilled water to remove the unreacted reagent.

Morphology and size of the silver nanoparticles

The morphology and the size of the synthesized AgNPs were characterized by ultraviolet–visible (UV–vis) spectroscopy (SpectraMax 340PC384 Microplate Reader, Molecular Devices,

CA, USA) and transmission electron microscopy (TEM) (Tecnai G2 20 S-TWIN Scanning, FEI, OR, USA). Ten TEM images of AgNPs were obtained, and particle sizes of the AgNPs were measured using computer software (Image J; National Institutes of Health, Bethesda, MD, USA). Surface zeta potential was characterized using Laser Doppler Micro electrophoresis (Zetasizer Nano ZS90, Malvern Panalytical, Malvern, UK).

Cell cytotoxicity

The cell cytotoxicity of the AgNPs was evaluated against human gingival fibroblast (HGF-1) and stem cells from human exfoliated deciduous teeth (SHED). Briefly, the HGF-1 cells or SHED (1×105/mL) were cultured in Dulbecco's modified eagle medium containing 10% foetal bovine serum and 1% penicillin for 24 h at 37 °C in a humidified atmosphere containing 5% carbon dioxide. The cells were then treated with various concentrations of AgNPs and $AgNO_3$. The cells with no treatment were the negative controls. After 24 h, the cells were washed with phosphate-buffered saline (PBS). Subsequently, 0.5 mg/mL MTT (MTT Cell Proliferation Assay Kit, Berkshire, UK) was applied and incubated for 4 h. The resulting crystal formazan was then solubilized in dimethyl sulfoxide for 10 min. The value of absorbance at 540 nm wavelength is measured as the activity of cells (Zhang et al. 2013). The relative viability in percentage of the cells treated with AgNPs or $AgNO_3$ was calculated from the ratio of average optical density of the test group over the average optical density of the negative control group. Half-maximal inhibitory concentration (IC_{50}) represents the concentration of the experimental solution that is required for 50% inhibition of the cell viability.

Antimicrobial test

The antimicrobial test of the AgNPs was conducted by determining the minimum inhibitory concentration (MIC) and minimum bactericidal concentration (MBC) towards *Streptococcus mutans* (ATCC 35668). The experimental groups were 4000 μg/mL AgNPs, 0.6% $AgNO_3$ (4000 μg/mL Ag^+; positive control), and water (negative control). In 96-well plates, 10 μL bacterial culture (McFarland 2) in brain heart infusion (BHI) broth was added with 100 mL serial two-fold dilution of experimental solutions.

The plates were then incubated under anaerobic conditions for 18 h. MIC determined from the wells did not exhibit visible bacterial growth. To determine the MBC value, 10 μL fluid was

pipetted from the wells in which the MIC was observed to BHI agar and incubated at 37 °C for 48 h. The samples from two concentrations above and one concentration below were also incubated.

Effect of the silver nanoparticles on cariogenic biofilm

This study received approval from the Institutional Review Board at the University of Hong Kong under process number IRB UW14-529.

Sound human third molars were collected with patients' consent. Twenty root dentine blocks with the thickness of 2mm were prepared. Each block without flaws or other defects was polished and cut into three specimens. Therefore, 60 specimens were prepared. The specimens were sterilized by autoclaving at 121 °C (Zhao et al. 2017b).

The specimens in three groups received topical application in three different treatments: group AgNPs, 4000 μg/mL AgNPs; group $AgNO_3$, 0.6% $AgNO_3$ (4000 μg/mL Ag^+); group W, deionized water. All solutions were applied to the specimen surface with a micro-brush (Micro applicator-regular, Premium Plus International Ltd., Hong Kong, China). After 10 min, the treated specimens were immersed in 1 mL *Streptococcus mutans* bacterial culture with BHI and 5% glucose (McFarland 2).

Subsequently, the specimens were incubated anaerobically at 37 °C. The specimens were collected at 6 h, 12 h, and 24 h.

Biofilm viability

The viability of bacteria in biofilm was assessed by confocal laser scanning microscopy (CLSM). The bacteria on the specimen surfaces were labelled in situ using two fluorescent probes: propodium iodide and SYTO-9 dye (LIVE/DEAD BacLight Bacterial viability kit, Molecular Probes, Eugene, OR, USA). CLSM (Fluoview FV 1000, Olympus, Tokyo, Japan) was used to obtain the images of labelled biofilm. The red-to-green ratio was calculated to denote the ratio of dead-to-live bacteria. A high ratio indicates the positive antimicrobial effect of the studied therapeutic agent.

Biofilm kinetics

The growth kinetics of the *Streptococcus mutans* biofilm was assessed by counting colony-forming units (CFU). *Streptococcus mutans* on the surface of each specimen were resuspended in 1 mL BHI broth using vortex flow for 1 min. BHI broth containing suspended bacteria was conducted serial tenfold dilution. Then, 10 μL bacteria suspension from each dilution was plated on blood agars. The agars were incubated at 37 °C for 48 h anaerobically, and then the CFUs were calculated.

Biofilm morphology

The biofilm morphology was assessed by scanning electron microscopy (SEM) (PHILIPS XL30 CP, Philips, Amsterdam, Netherlands). The specimens were fixed by 2.5% glutaraldehyde for 4 h at 4 °C followed by 1% (vol/vol) PBS. Then the fixed specimens experienced dehydrated using 70%, 80%, 90% and 100% ethanol. After dehydration in a series of ethanol, specimens were dried in a desiccator and sputter-coated with gold before examination.

Lactic acid production

Amount of lactic acid produced by biofilm was measured to estimate the cariogenicity of biofilm. Dentine blocks were collected after 24 h biofilm challenge and washed twice with PBS. Blocks were immersed in 1.5 mL buffered peptone water supplemented with 0.2% sucrose and incubated at 37 °C in 5% CO2 for 3 h. Supernatant was collected from each well and centrifuged at 10,000 × g for 15 min at 4 °C to remove insoluble material. The concentration of lactate in supernatant were quantified with lactate dehydrogenase (LDH) enzymatic method by using LDH activity assay kit (Wang et al. 2019). Six blocks were tested for each group.

Polysaccharide production

Water-insoluble polysaccharide of biofilm was tested to show the virulence of biofilm. Biofilm after 24 h culture was collected from dentine surface by vortex in 1 mL PBS for 1 min, followed by centrifugation. The precipitated cells were then washed twice and resuspended in 200 μL of deionized water followed by adding 200 μL of 5% phenol solution and 1 mL of 95–97% sulfuric acid. After incubation at room temperature for 30 min, 200 μL of the solution was

transferred into a 96-well plate and OD490 nm was determined with the microplate reader (Wang et al. 2019). Six blocks were tested for each group.

Colour test

Colour assessments were taken before treatment of experimental groups (T0) and after *Streptococcus mutans* biofilm challenge over 24 h (T1). The colours were examined with the VITA Easyshade Advance Portable Dental Spectrophotometer (VITA Zahnfabrik GmbH, Bad Säckingen, Germany).

Prior to measuring the colour of the blocks, an infection control shield was applied to the VITA Easyshade Advance 4.0 probe tip and the instrument calibrated. The blocks were checked under microscope (x10) for cleanliness and any surface contaminations were removed from the surface of a tooth prior to measurement. The probe tip was positioned firmly and entirely on the blocks.

The colour of each specimen was elucidated according to the Commission International del'Eclairage L* a* b* colour system. L* axis represented lightness ranged from black (0) to white (100), a* axis described red (+a*) to green (-a*), and the b* axis represented yellow (+b*) to blue (-b*). Total colour change (△E) between T0 and T1 was calculated based on the equation:

$$\Delta E^* = \sqrt{[(\Delta L)^2 + (\Delta a)^2 + (\Delta b)^2]}$$

Statistical analysis

Normal distribution was assessed for all data by the Shapiro-Wilk test ($p>0.05$). Parametric t-test was used to compare MIC, MBC, and IC_{50} between AgNPs and $AgNO_3$. Pairwise t-test was employed to assess the L*, a*, and b* values between T0 and T1 within each group. One-way ANOVA with Bonferroni multiple comparison tests was used to compare the values of log CFU and red-to-green ratio among different groups. All data were analysed with IBM SPSS V20.0 software (IBM Corporation, Armonk, NY, USA) and the level of significance was set at 5%.

Results

Figure 1 (a) shows the synthesized AgNPs colloidal suspension which represents the formation of spherical monodispersed AgNPs. The average particle size was 17.38 ± 7.26 nm in diameter (Figure 1 (b)). The AgNPs synthesized with chitosan and EGCG had surface plasmon resonance band at 402 nm in UV–vis absorption spectrum (Figure 1 (c)), the narrow peak indicated the narrow particle size range. The surface zeta potential was 47.3 ± 5.72 mV (Figure 1 (d)) indicating good stability of AgNPs colloidal.

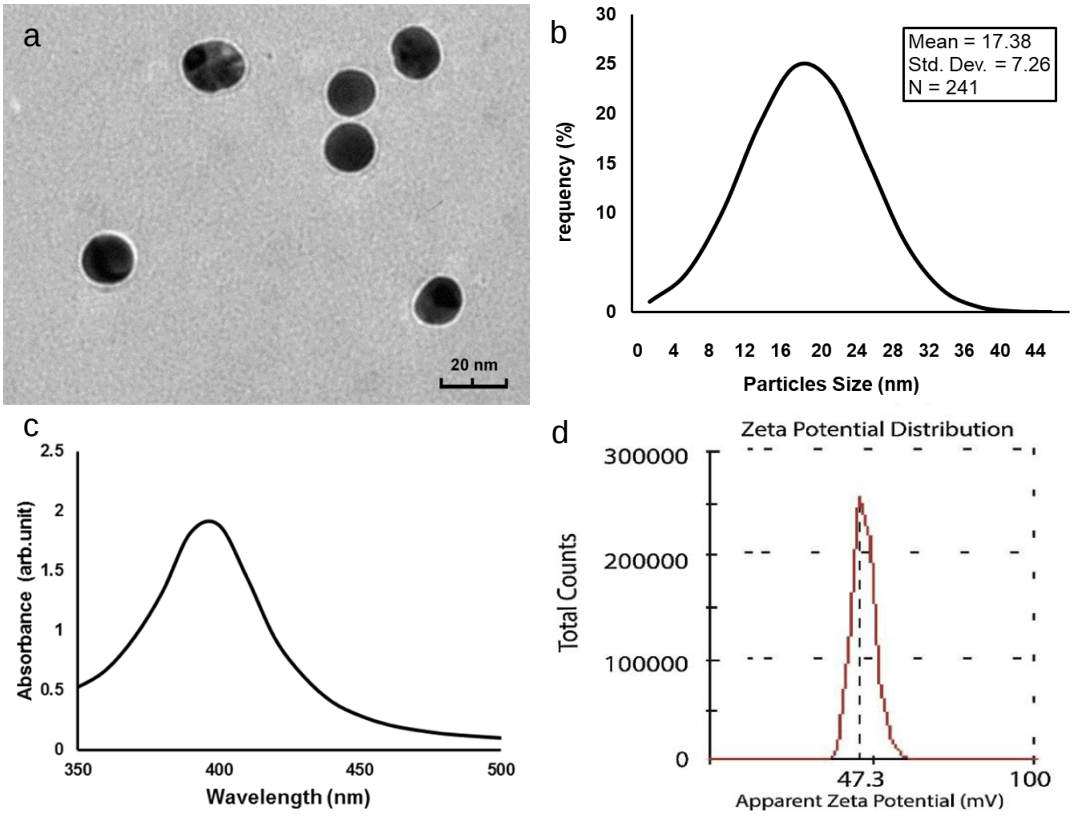

Figure 1 (a) TEM image, (b) size distribution, (c) UV–vis spectrum and (d) zeta potential distribution of AgNPs

IC_{50} of AgNPs against SHED and HGF-1 were significantly higher than those of $AgNO_3$ ($p < 0.05$, Table 1), while the MIC and MBC values of AgNPs against *S. mutans* were significantly lower than those of $AgNO_3$ ($p < 0.05$, Table 1).

Table 1 The IC_{50}, MIC and MBC of AgNPs and $AgNO_3$

	IC_{50} against SHED(μg/mL)	IC_{50} against HGF-1(μg/mL)	MIC against *S. mutans* (μg/mL)	MBC against *S. mutans* (μg/mL)
AgNPs	68.02 ± 24.48	44.88 ± 11.39	32.22 ± 7.34	63.33 ± 11.73
$AgNO_3$	9.54 ± 6.63	11.53 ± 6.96	48.89 ± 15.11	85.00 ± 20.77
p value	0.02	<0.001	0.01	0.02

The red-to-green ratios, calculated from CLSM images, were significantly higher in the AgNPs group than those in the $AgNO_3$ group and water group at 6, 12, and 24 h (Table 2, $p < 0.01$). CLSM images revealed consistent results with red-to-green ratio, which indicated that proportion of dead bacteria in the AgNPs group was higher than those in $AgNO_3$ and water groups at 6, 12, and 24 h (Figure 2).

	Red/Green		
	6 h	12 h	24 h
AgNPs [1]	1.36 ± 0.28	0.84 ± 0.09	0.77 ±0.19
$AgNO_3$ [2]	0.70 ± 0.13	0.61 ± 0.16	0.39 ±0.22
Water [3]	0.36 ± 0.14	0.35 ± 0.09	0.23 ±0.12
p value	$p < 0.001$	$p < 0.001$	$p = 0.006$
Multiple comparison	1 > 2, 3	1 > 2, 3	1 >2, 3

Table 2 Red-to-green ratio of experimental groups at 6 h, 12 h and 24 h

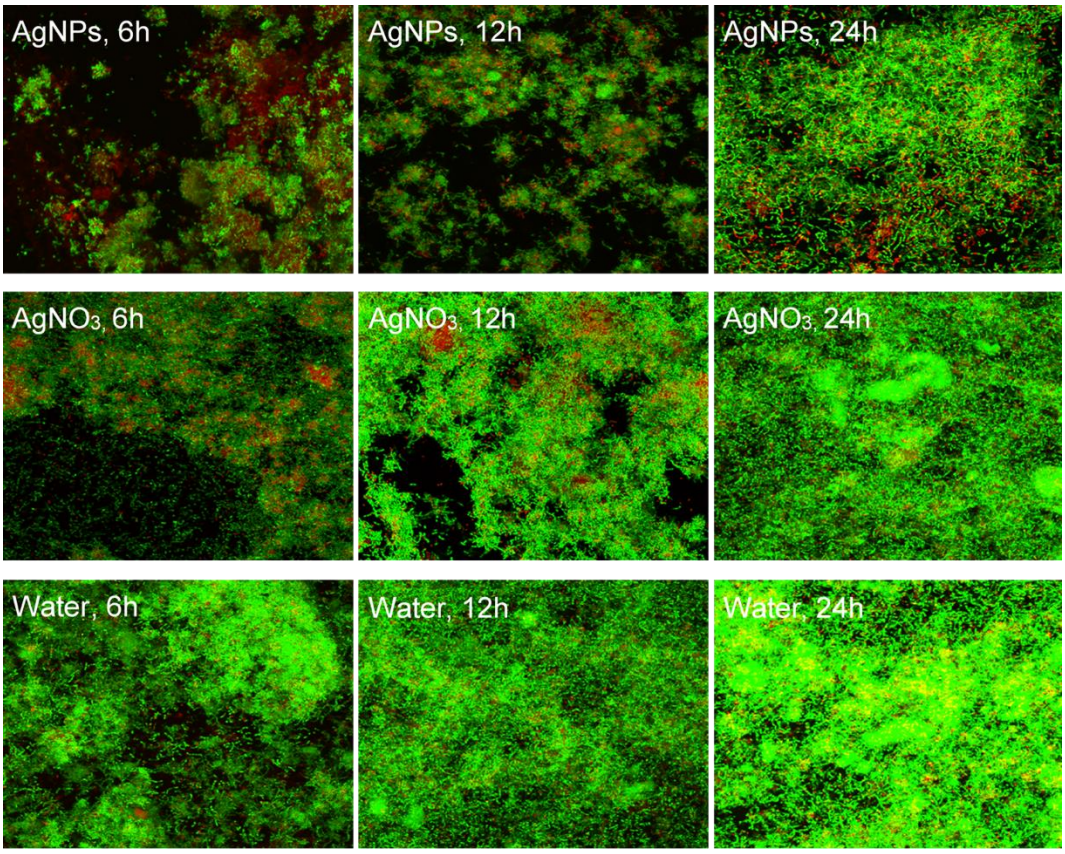

Figure 2 CLSM images (×100) of *S. mutans* biofilm of AgNPs, $AgNO_3$ and water groups at 6 h, 12 h and 24 h

Log CFUs of AgNPs were the lowest among AgNPs, $AgNO_3$ and water groups at all time points ($p < 0.001$, Table 3).

	Log CFUs		
	6 h	12 h	24 h
AgNPs [1]	4.26 ± 0.37	5.85 ± 0.49	6.23 ± 0.15
$AgNO_3$ [2]	5.67 ± 0.42	7.05 ± 0.11	7.16 ± 0.12
Water [3]	6.84 ± 0.81	7.73 ± 0.43	7.91 ± 0.03
p value	$p < 0.001$	p < 0.001	p < 0.001
Multiple comparison	1 < 2 < 3	1 < 2 < 3	1 < 2 < 3

Table 3 Log CFUs in AgNPs, $AgNO_3$ and water groups at 6 h, 12 h and 24 h

SEM images did not show noticeable bacteria accumulation on root dentine surface in group AgNPs at all time points (Figure 3), while obvious biofilms were formed in both the $AgNO_3$ and water groups after 24 h.

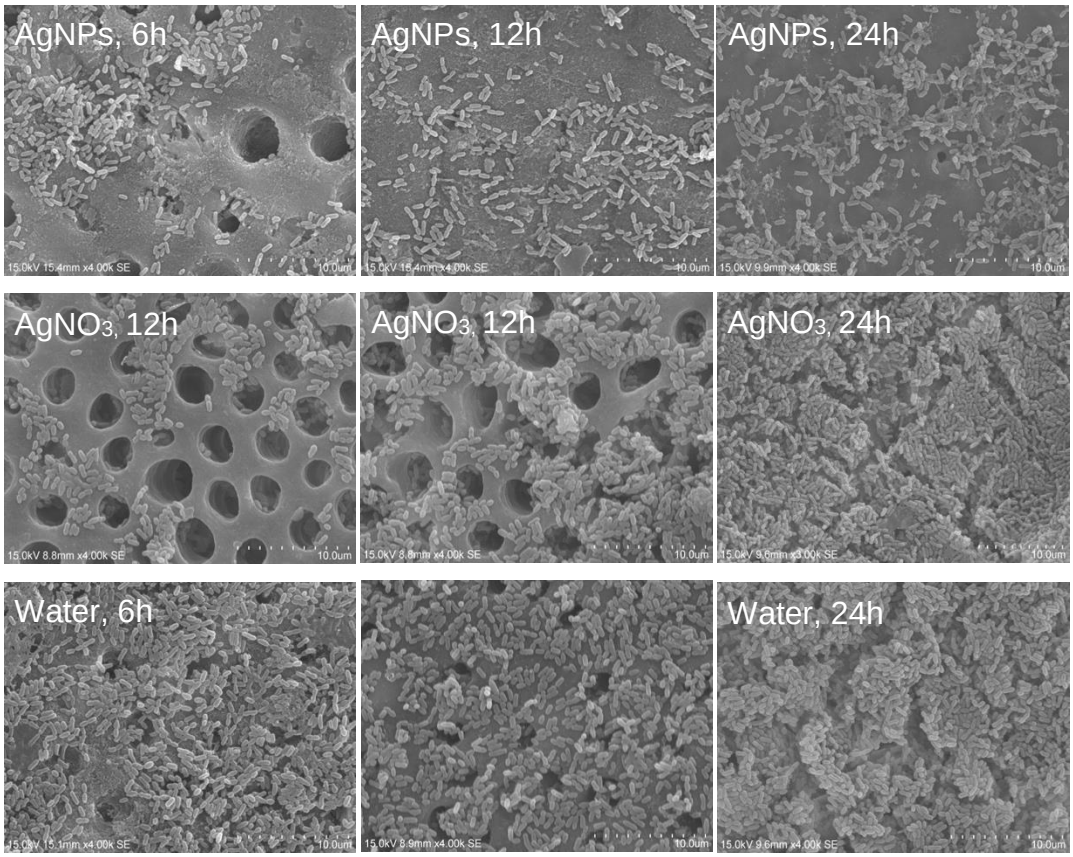

Figure 3 SEM images of *S. mutans* biofilm of AgNPs, $AgNO_3$ and water groups at 6 h, 12 h and 24 h

Lactic acid production and polysaccharides production by *S. mutans* biofilms were showed in Table 4. The acid production in AgNPs group was significantly lower than that in $AgNO_3$ group and water group ($p < 0.001$). The production of polysaccharides in AgNPs group was significantly lower than $AgNO_3$ group and water group ($p < 0.001$).

	Lactic acid (mM)	Polysaccharide (mg/mL)
AgNPs [1]	1.98 ± 0.17	3.35 ± 2.10
$AgNO_3$ [2]	2.17 ± 0.19	5.48 ± 1.42
Water [3]	2.38 ± 0.18	7.78 ± 1.48
p value	$p < 0.001$	$p < 0.001$
Multiple comparison	1 < 2 < 3	1 < 2 < 3

Table 4 The concentration of lactic acid production water-insoluble polysaccharide production in *S. mutans* biofilm after 24 h

The values relating to the chromatic coordinates L* a* b* of the three groups are presented in Table 5. For the intragroup analysis, a significant collapse in the lightness (L*) values of from 60.40 ± 2.98 to 28.96 ± 3.21 ($p < 0.001$) was observed in the $AgNO_3$ group after biofilm challenge, while the AgNPs group (p=0.25) and water group (p = 0.06) displayed similar values of L* between two time points. The slight decline in the values of a* among all three groups after biofilm growth was distinctly witnessed, separately ($p < 0.05$). A distinguished drop was detected from 18.39 ± 0.73 to 7.15 ± 2.08 ($p < 0.001$) of b* values of the $AgNO_3$ group. △E between the AgNPs group (5.80 ± 2.65) and water group (4.65 ± 1.67) showed no significant difference (p = 0.64) in multiple comparisons. △E value of the $AgNO_3$ group (33.52 ± 2.17) was significantly higher than **that of the AgNPs and water ($p < 0.001$) groups, respectively.**

Group	Coordinates	Before	After	*p* value
AgNPs	L*	60.04 ± 2.07	57.22 ± 5.09	0.25
	a*	7.75 ± 0.66	7.12 ± 0.55	0.04
	b*	21.05 ± 0.68	18.53 ± 1.81	0.01
$AgNO_3$	L*	60.40 ± 2.98	28.96 ± 3.21	< 0.001
	a*	7.55 ± 0.85	5.89 ± 1.40	0.01
	b*	18.39 ± 0.73	7.15 ± 2.08	< 0.001
Water	L*	61.55 ± 4.31	58.48 ± 6.00	0.06
	a*	9.58 ± 0.66	8.26 ± 0.80	0.01
	b*	24.02 ± 2.53	22.04 ± 2.54	0.003

Table 5 Values of L* a* b* coordinates of the experimental groups

Discussion

We developed a novel biocompatible and antibacterial AgNPs for dental use in this study. This is the first study to use EGCG as the reducing agent to synthesize colloidal AgNPs for dental use. The results of this study demonstrated that synthesized AgNPs had promising antibacterial properties against *S. mutans* on root dentine surface with high biocompatibility. The AgNPs have potential to be used in caries management through controlling of cariogenic biofilm growth on tooth surface.

S. mutans is a major cariogenic bacteria in the development of caries. *S. mutans* are highly acidogenic and can produce short-chain carboxylic acids like acetic acid; the acid will dissolve dental hard tissue (Brailsford et al. 2001). In addition, *S. mutans* can ferment sucrose and produce extracellular polysaccharides which enhance bacterial adherence to tooth surfaces to facilitate biofilm formation. *S. mutans* biofilm is one of the most common microbial models used in caries research (Yu et al. 2017). However, mono-species biofilms in a microplate system are very different in both survival and pathogenic potential from the complex in vivo multispecies plaque biofilms. Therefore, the results cannot be extrapolated to the in vivo situation directly and caution should be exercised in their interpretation.

The results of the present study revealed that AgNPs showed a superior and longer antimicrobial effect against *S. mutans* than that of $AgNO_3$ at the same concentration of silver. In addition, biofilms in AgNPs group was revealed with lowest level of acidic acid and polysaccharides production ($p < 0.001$). Lactic acid stands for 70% of the organic acids produced in oral biofilm and is considered as a key factor leading to demineralisation of the teeth (Featherstone 2000). Polysaccharides is another important virulence factor contribute to formation of the biofilm (Bowen and Koo 2011). AgNPs and silver ions (Ag^+) can interfere with the respiratory chain in the bacterial mitochondria, resulting in cell death. However, AgNPs can provide a large surface area for contact with bacteria, which may facilitate silver particles attaching to and penetrating the cell membrane of the bacteria (Wong and Liu 2010).

The synergistic effect of AgNPs occurs when these particles are combined with other natural and synthetic compounds (Durán et al. 2016). EGCG is the major polyphenol present in green tea. The antimicrobial mechanism of EGCG is mainly due to its inhibitory effects on glucosyltransferases of *S. mutans*, consequently affecting the initial adherence of bacteria and therefore destroying the formation and integrity of oral biofilms. EGCG has also been shown to reduce the rate of acid production by *S. mutans* and intervenes with the growth rate of *S. mutans*. Chitosan is a well-known capping agent in nanomedicine used to deliver therapeutic drugs, proteins, and genes. It has remarkable affinity to bacterial membrane, which prolongs retention and contributes to a high uptake of the nanoparticles (Moulton et al. 2010). AgNPs capped into chitosan was researched that has strong antibacterial activity even for drug-resistant bacteria (Liang et al. 2016). Chitosan has also expressed the capability to reduce the plaque index and the vitality of the plaque flora of *S. mutans* (Bae et al. 2006). Studies demonstrated that AgNPs have a slower dissolution rate when compared to silver salts, which leads to a continuous release of silver ions (Ho et al. 2010). This is why AgNPs have a longer antimicrobial effect when compared to $AgNO_3$.

This study revealed that AgNPs synthesized by EGCG have lower cytotoxicity on HGF-1 and SHED when compared to $AgNO_3$ (Table 4.1), which indicates that AgNPs have low toxicity to oral mucosa as well as the differentiation of stem cells. This mimics the situation that when AgNPs were released into the oral environment, local effects are mostly manifested on pulp, gingival and oral mucosa cell (Lee et al. 2015). Toxicity is always a major concern of AgNPs. One study found that silver harms or kills bacteria in the same concentration range that harms human cells (Greulich et al. 2012). The generation of ROS upon exposure of cells to nanoparticles is a major contributor to the toxicity of AgNPs (Greulich et al. 2011).

EGCG is a tea extract that contains potential healthy traits, including antioxidant, antimicrobial, antidiabetic, anti-inflammatory, and cancer preventive properties (Du et al. 2012). As an antioxidant, EGCG has been demonstrated to inhibit the ROS inside cells effectively (Skebo et al. 2007) and to counteract the harmful effects of free radicals and protect structural integrity of the protein. A previous study found that the cell viability was positively affected by tea extract, potentially through the antioxidants protecting the cells (Moulton et al. 2010). Moreover, the study

authors also found that the cells can internalize nanoparticles developed by tea extract, without cellular morphology changes (Moulton et al. 2010). Furthermore, a study demonstrated that the disruption in cell viability caused by nanoparticles could be prevented by pre-treatment or co-treatment with an antioxidant (Braydich-Stolle et al. 2009). Thus, we assume that EGCG remaining on the surface of the AgNPs will inhibit the ROS and therefore protect the cell surface. We also found that the dentine surface in the AgNPs group showed little colour changes even after biofilm challenge, which is quite different from the black stain caused by Ag^{+} solution. ΔE of AgNPs group and water group are 5.80 and 4.65, which are slightly higher than the perceptibility threshold (3.7), showing a slightly brown in appearance (Zhao et al. 2017a). This brownish can be due to incipient lesions on the dentine (Kleter 1998). The promising optoelectronic properties of AgNPs are due to surface plasmon resonance, which may arise from the confinement of the electrons to dimensions smaller than the wavelength of light, the acceleration of electron conduction by the electric field of incident radiation, and the presence of restoring forces due to induced polarization in both the particles and the surrounding medium (Ravindran et al. 2013). The smaller nanospheres primarily absorb light, while larger spheres increase scattering and absorption peaks are broaden and shift towards longer wavelengths (Noronha et al. 2017).

Apart from optical property, particle size of the nanoparticles is also related with both antimicrobial and biocompatible properties. It has been reported that the toxicity of 20–80 nm silver nanoparticles was assigned to the release of silver ions, whereas 10 nm silver nanoparticles proved to be more toxic (Raza et al. 2016). This is due to the smaller nanoparticles had more efficient cell-particle contact than 20–80 nm silver nanoparticles, leading to higher intracellular bioavailability of silver (Durán et al. 2015). While study also showed size-dependent antibacterial activities of AgNPs against oral anaerobic pathogenic bacteria, the smaller the size, the better antibacterial property (Lu et al. 2013). The particle size of AgNPs in our study is around 20 nm, which compromised both the biocompatible and antimicrobial properties in an acceptable level.

Conclusion

Biocompatible and antibacterial AgNPs developed using EGCG can be potentially useful in dentistry.

Ethical approval

This study received approval from the Institutional Review Board at the University of Hong Kong under process number IRB UW14-529.

Acknowledgements

This study was supported by the Health and Medical Research Fund (HMRF) 17160402 of the Food and Health Bureau of the Hong Kong Government and General Research Fund (GRF) 17100218 of the Research Grant Council, Hong Kong.

References

Bae K, Jun E, Lee S, Paik D, Kim J. 2006. Effect of water-soluble reduced chitosan on streptococcus mutans , plaque regrowth and biofilm vitality. Clin Oral Invest. 10(2):102-107.

Bhattacharya R, Mukherjee P. 2008. Biological properties of "naked" metal nanoparticles. Advanced Drug Delivery Reviews. 60(11):1289-1306.

Bowen WH, Koo H. 2011. Biology of streptococcus mutans-derived glucosyltransferases: Role in extracellular matrix formation of cariogenic biofilms. Caries Research. 45(1):69-86.

Brailsford SR, Shah B, Simons D, Gilbert S, Clark D, Ines I, Adams SE, Allison C, Beighton D. 2001. The predominant aciduric microflora of root-caries lesions. Journal of Dental Research. 80(9):1828-1833.

Braydich-Stolle L, Schaeublin N, Murdock R, Jiang J, Biswas P, Schlager J, Hussain S. 2009. Crystal structure mediates mode of cell death in tio 2 nanotoxicity. J Nanopart Res. 11(6):1361-1374.

Carlson C, Hussain SM, Schrand AM, K. Braydich-Stolle L, Hess KL, Jones RL, Schlager JJ. 2008. Unique cellular interaction of silver nanoparticles: Size-dependent generation of reactive oxygen species. The journal of physical chemistry B. 112(43):13608-13619.

Cassee FR, van Balen EC, Singh C, Green D, Muijser H, Weinstein J, Dreher K. 2011. Exposure, health and ecological effects review of engineered nanoscale cerium and cerium oxide associated with its use as a fuel additive. Critical reviews in toxicology. 41(3):213-229.

Chauhan K, Sharma R, Dharela R, Chauhan GS, Singhal RK. 2016. Chitosan-thiomer stabilized silver nano-composites for antimicrobial and antioxidant applications. RSC advances. 6(79):75453-75464.

Du X, Huang X, Huang C, Wang Y, Zhang Y. 2012. Epigallocatechin-3-gallate (egcg) enhances the therapeutic activity of a dental adhesive. Journal of dentistry. 40(6):485-492.

Durán N, Durán M, De Jesus MB, Seabra AB, Fávaro WJ, Nakazato G. 2016. Silver nanoparticles: A new view on mechanistic aspects on antimicrobial activity. Nanomedicine: Nanotechnology, Biology and Medicine. 12(3):789-799.

Durán N, Silveira CP, Durán M, Martinez DST. 2015. Silver nanoparticle protein corona and toxicity: A mini-review. Journal of nanobiotechnology. 13(1):55.

Featherstone JD. 2000. The science and practice of caries prevention. The Journal of the American dental association. 131(7):887-899.

Ferrazzano GF, Amato I, Ingenito A, Zarrelli A, Pinto G, Pollio A. 2011. Plant polyphenols and their anti-cariogenic properties: A review. Molecules. 16(2):1486-1507.

Greulich C, Braun D, Peetsch A, Diendorf J, Siebers B, Epple M, Köller M. 2012. The toxic effect of silver ions and silver nanoparticles towards bacteria and human cells occurs in the same concentration range. RSC advances. 2(17):6981-6987.

Greulich C, Diendorf J, Simon T, Eggeler G, Epple M, Köller M. 2011. Uptake and intracellular distribution of silver nanoparticles in human mesenchymal stem cells. Acta biomaterialia. 7(1):347-354.

Griffin S, Griffin P, Swann J, Zlobin N. 2004. Estimating rates of new root caries in older adults. Journal of dental research. 83(8):634-638.

Ho CM, Yau SKW, Lok CN, So MH, Che CM. 2010. Oxidative dissolution of silver nanoparticles by biologically relevant oxidants: A kinetic and mechanistic study. Chemistry–An Asian Journal. 5(2):285-293.

Hussain S, Khan Z. 2014. Epigallocatechin-3-gallate-capped ag nanoparticles: Preparation and characterization. Bioprocess and biosystems engineering. 37(7):1221-1231.

Kassebaum N, Bernabé E, Dahiya M, Bhandari B, Murray C, Marcenes W. 2015. Global burden of untreated caries: A systematic review and metaregression. Journal of dental research. 94(5):650-658.

Kidd E, Fejerskov O. 2004. What constitutes dental caries? Histopathology of carious enamel and dentin related to the action of cariogenic biofilms. Journal of dental research. 83(1_suppl):35-38.

Kleter G. 1998. Discoloration of dental carious lesions (a review). Archives of oral biology. 43(8):629-632.

Lee Y, Ahn J-S, Yi Y-A, Chung S-H, Yoo Y-J, Ju S-W, Hwang J-Y, Seo D-G. 2015. Cytotoxicity of four denture adhesives on human gingival fibroblast cells. Acta Odontologica Scandinavica. 73(2):87-92.

Liang D, Lu Z, Yang H, Gao J, Chen R. 2016. Novel asymmetric wettable agnps/chitosan wound dressing: In vitro and in vivo evaluation. ACS applied materials & interfaces. 8(6):3958-3968.

Lu Z, Rong K, Li J, Yang H, Chen R. 2013. Size-dependent antibacterial activities of silver nanoparticles against oral anaerobic pathogenic bacteria. Journal of Materials Science: Materials in Medicine. 24(6):1465-1471.

Moulton MC, Braydich-Stolle LK, Nadagouda MN, Kunzelman S, Hussain SM, Varma RS. 2010. Synthesis, characterization and biocompatibility of "green" synthesized silver nanoparticles using tea polyphenols. Nanoscale. 2(5):763-770.

Noronha VT, Paula AJ, Duran G, Galembeck A, Cogo-Mueller K, Franz-Montan M, Duran N. 2017. Silver nanoparticles in dentistry. Dental Materials. 33(10):1110-1126.

Ravindran A, Chandran P, Khan SS. 2013. Biofunctionalized silver nanoparticles: Advances and prospects. Colloids and Surfaces B: Biointerfaces. 105:342-352.

Raza MA, Kanwal Z, Rauf A, Sabri AN, Riaz S, Naseem S. 2016. Size-and shape-dependent antibacterial studies of silver nanoparticles synthesized by wet chemical routes. Nanomaterials. 6(4):74.

Regiel A, Irusta S, Kyzioł A, Arruebo M, Santamaria J. 2012. Preparation and characterization of chitosan–silver nanocomposite films and their antibacterial activity against staphylococcus aureus. Nanotechnology. 24(1):015101.

Skebo JE, Grabinski CM, Schrand AM, Schlager JJ, Hussain SM. 2007. Assessment of metal nanoparticle agglomeration, uptake, and interaction using high-illuminating system. International journal of toxicology. 26(2):135-141.

Wang H, Wang S, Cheng L, Jiang Y, Melo MAS, Weir MD, Oates TW, Zhou X, Xu HH. 2019. Novel dental composite with capability to suppress cariogenic species and promote non-cariogenic species in oral biofilms. Materials Science and Engineering: C. 94:587-596.

Wong KK, Liu X. 2010. Silver nanoparticles—the real "silver bullet" in clinical medicine? MedChemComm. 1(2):125-131.

Wu CD, Wei G-X. 2002. Tea as a functional food for oral health. Nutrition (Burbank, Los Angeles County, Calif). 18(5):443-444.

Yu OY, Zhao IS, Mei ML, Lo EC-M, Chu C-H. 2017. Dental biofilm and laboratory microbial culture models for cariology research. Dentistry journal. 5(2):21.

Zhang K, Cheng L, Imazato S, Antonucci JM, Lin NJ, Lin-Gibson S, Bai Y, Xu HH. 2013. Effects of dual antibacterial agents mdpb and nano-silver in primer on microcosm biofilm, cytotoxicity and dentine bond properties. Journal of dentistry. 41(5):464-474.

Zhao IS, Mei ML, Burrow MF, Lo EC-M, Chu C-H. 2017a. Effect of silver diamine fluoride and potassium iodide treatment on secondary caries prevention and tooth discolouration in cervical glass ionomer cement restoration. International journal of molecular sciences. 18(2):340.

Zhao IS, Mei ML, Burrow MF, Lo EC-M, Chu C-H. 2017b. Prevention of secondary caries using silver diamine fluoride treatment and casein phosphopeptide-amorphous calcium phosphate modified glass-ionomer cement. Journal of dentistry. 57:38-44.